

Cooling, Physical Scales and Topology

Margarita García Pérez^{1,2},
Owe Philipsen^{2,3}
and Ion-Olimpiu Stamatescu^{2,4}

¹ Departamento de Física Teórica, Universidad Autónoma de Madrid,
Canto Blanco, 28049 Madrid, Spain

²Institut für Theoretische Physik, Philosophenweg 16,
D-69120, Heidelberg, Germany

³Theory Division, CERN, CH-1211, Geneva 23, Switzerland

⁴FEST, Schmeilweg 5, D-69118, Heidelberg, Germany

Abstract

We develop a cooling method controlled by a physical *cooling radius* that defines a scale below which fluctuations are smoothed out while leaving physics unchanged at all larger scales. We apply this method to study topological properties of lattice gauge theories, in particular the behaviour of instantons, dislocations and instanton–anti-instanton pairs. Monte Carlo results for the $SU(2)$ topology are presented. We find that the method provides a means to prevent instanton–anti-instanton annihilation under cooling. While the instanton sizes are largely independent from the smoothing scale, the density and pair separations are determined by the particular choice made for this quantity. We discuss the questions this raises for the “physicality” of these concepts.

CERN-TH 98-380

December 1998

arXiv:hep-lat/9812006v2 11 Dec 1998

1 Introduction

Beyond providing quantitative estimates for various physical parameters like masses and decay constants, Monte Carlo simulations of lattice gauge theories are increasingly involved in obtaining a physical picture of the structure of quantum field theories, such as the quantum vacuum and its topological properties. Such analyses are hampered by the ultraviolet fluctuations of the fields at scales comparable with the lattice spacing. A typical example of these problems is the scaling behaviour of the $SU(N = 2, 3)$ topological susceptibility which, for the commonly used lattice actions, turns out to be spoiled by the presence of topological fluctuations at the scale of the cut-off (dislocations).

The need to improve the continuum approach of physical quantities has motivated the development of techniques to smooth out the UV, cut-off-dependent, structure of the configurations before measuring on them the quantities of interest, be these physical parameters like masses or features of the quantum vacuum. Apart from the improvement of lattice actions there are essentially two approaches that have been taken to realize this program:

- (i) preparing operators that are insensitive to UV fluctuations, and
- (ii) smoothing the fields themselves.

For example, by smearing the spatial link variables [1] on fixed time slices one constructs spatially extended operators with increased overlap onto the physical states, and thereby also achieves (i). This procedure preserves the transfer matrix and hence the physical content. It has been successfully applied to potential and spectrum measurements.

Smearing of the link variables can also be performed in an isotropic way, i.e. involving also the links in the time direction. When this is done on all links of the lattice before the measurements, it amounts to (ii). In this case locality and hence the transfer matrix interpretation are lost at the level of the original lattice. Isotropic smearing has been found to be useful to minimize UV renormalization effects of the charge operator in measurements of the topological susceptibility [2] and other properties of the gauge theory vacuum [3]. However, it is not always clear if and to which limit the procedure converges [4].

A special case of the second approach is cooling [5]. It consists of an iterative, local minimization of the action, which proceeds sweep-wise and converges to configurations fulfilling the classical (Euclidean) equations of motion. In the case of continuum gauge theories, these are configurations characterized by the topological sector Q obeying $S = |Q|S_1$, where $S_1 = 8\pi^2/g^2$ is the action of one instanton. Hence, up to scaling violations associated with the lattice discretization and assuming that topology preserves its meaning away from the semi-classical approximation, cooling should reveal the topological sector to which the original configuration belongs.

Different smoothing techniques such as smearing [3], cooling [6]-[15] and inverse block-

ing [16, 17] have also been applied in investigating whether gauge theory configurations can be described as instanton ensembles. Although results obtained for the topological susceptibility seem to be procedure-independent (i.e. they agree within 10%), the situation is far less satisfactory for the determination of the instanton size distribution or the instanton density, which is mostly due to ambiguities in extracting the instanton content from the Monte Carlo configurations (for recent reviews, see [18, 19]).

Cooling is known to proceed as a diffusion process in the sense that the length scale up to which it smoothes the configurations grows with the number of iterations [20, 21]. There are two problematic features that are common to standard cooling procedures:

1. In general the physical spectrum cannot be extracted from correlation distances shorter than the “cooling radius” to which smoothing has advanced. For example, the string tension extracted from a given pair of time slices rapidly diminishes as cooling proceeds (for discussions of this point, see below and [10, 22]).
2. Instanton–anti-instanton pairs, unlike superpositions of only instantons (I) or only anti-instantons (A), do not represent saddle points of the action. They belong to the topologically trivial sector and can have any action between $2S_1$ and 0. Consequently they are indistinguishable from trivial topological fluctuations and are removed by the cooling process. On the other hand, since in many instanton-based models they are conjectured to be relevant for important physical effects (for a review see [23]) one would like to investigate if and how they are represented in the configurations.

The question then is whether it is possible to apply a well defined amount of cooling, such that the configurations do not lose their physical properties at the length scales one is studying, but have become smooth enough to allow their identification. With the present cooling techniques, a well defined criterion to achieve this is lacking. The amount of cooling employed has to be fixed by subjectively judging when the configurations appear smooth enough to extract topological quantities¹. In this paper, we introduce a systematic way of determining the cooling radius and relating it directly to a physical (continuum) length scale. This allows a smoothing of the fields up to a predefined scale, leaving all properties on larger scales untouched, and hence avoids the necessity of monitoring the cooling process, with all uncertainties involved in it.

The procedure we shall introduce and discuss here is to let cooling saturate according to a *local* criterion. Following a suggestion by Niedermayer [24], the local updating of links in the direction of minimization of the local action is only performed if the equations of motion are locally violated by more than a threshold δ (see section 2). As a result, cooling

¹ We stress that this difficulty does not affect the topological susceptibility, measured on cooled configurations, since I-A annihilation does not change the topological sector Q .

will only proceed where the links are still far from the local minimum, and stop when the structure has everywhere approached the classical solution to a degree related to δ . As we will see, this allows to preserve the string tension above a distance given by the cooling radius and provides a natural lattice implementation of the valley method constraint to prevent instanton–anti-instanton annihilation (see e.g. [25]).

In section 2 we introduce our cooling algorithm. The problem of relating the cooling radius to a continuum length scale will be discussed in section 3. In section 4 we test the effect of the algorithm on small instantons and I-A pairs, whereas section 5 contains results for the topological susceptibility and the properties of the instanton ensemble. Finally, section 6 is reserved for conclusions and outlook.

The numerical results presented in this work have been obtained on the lattices indicated in Table 1. The $12^3 \times 36$ lattice has periodic boundary conditions in all four

Lattice	b.c.	β	a (fm)	Confs.	Sep. sweeps	Therm. sweeps
$12^3 \times 36$	Periodic	2.4	0.12	800	100	20000
24^4	Twist in time	2.6	0.06	350	200	20000

Table 1: *Simulation parameters*

directions, while the 24^4 lattice has twisted boundary conditions in the time direction, with twist $\vec{k} = (1, 1, 1)$. The large “time” extension and the twisted boundary conditions have been adopted in order to suppress finite-size effects peculiar to the $|Q| = 1$ charge sector [26, 27, 12]. For the generation of configurations, we use the Wilson action.

2 Improved cooling and restricted improved cooling

In [11, 12] we introduced “improved cooling” (IC), based on a lattice action with improved scale invariance, as a well defined method to systematically eliminate UV noise and dislocations while preserving the topological charge associated with instantons above a certain size threshold $\rho_0 \sim 2.3a$. Here we shall recall some results of IC that are relevant for our discussion.

IC uses an action whose instanton solutions are scale-invariant for sizes beyond the *dislocation threshold* ρ_0 of the order of the lattice spacing a . From a tree-level analysis [27] one can determine a five-loop combination

$$S_{m,n} = \frac{1}{m^2 n^2} \sum_{x,\mu,\nu} \text{Re Tr} \left(1 - \begin{array}{c} x+n\nu \\ \begin{array}{|c|} \hline \begin{array}{c} \xrightarrow{\quad} \\ \xrightarrow{\quad} \\ \xrightarrow{\quad} \end{array} \\ \hline \end{array} \\ x \qquad \qquad \qquad x+m\mu \end{array} \right)$$

$$S = \sum_{i=1}^5 c_i S_{m_i, n_i}. \quad (1)$$

$(m_i, n_i) = (1, 1), (2, 2), (1, 2), (1, 3), (3, 3)$ for $i = 1, \dots, 5$ and:

$$\begin{aligned} c_1 &= (19 - 55 c_5)/9, & c_2 &= (1 - 64 c_5)/9, \\ c_3 &= (-64 + 640 c_5)/45, & c_4 &= 1/5 - 2 c_5, \end{aligned} \quad (2)$$

which has no tree-level $\mathcal{O}(a^2)$ and $\mathcal{O}(a^4)$ corrections at any c_5 . We have chosen $c_5 = 1/20$, which appears to minimize the $\mathcal{O}(a^6)$ corrections for instanton configurations.

The cooling algorithm is derived from the equations of motion

$$U_\mu(x)W_\mu(x)^\dagger - W_\mu(x)U_\mu(x)^\dagger = 0, \quad (3)$$

where W is the sum of staples connected to the link $U_\mu(x)$ in Eq. (1). For $SU(2)$, for instance, cooling amounts to the substitution (for clarity we drop the indices when possible):

$$U \rightarrow U' = V = W/\|W\|, \quad \|W\|^2 = \frac{1}{2}\text{Tr}(WW^\dagger). \quad (4)$$

Above the *dislocation threshold*, $\rho_0 \simeq 2.3a$, instantons are completely stable to any degree of cooling (at least if they are not affected by finite-size effects; see [12] for a discussion of this point). The corresponding *improved charge density* using the same combination of loops leads to an integer charge already after a few cooling sweeps.

We now supplement this cooling procedure by imposing the constraint that only those links be updated, which violate the equation of motion by more than some $\tilde{\delta}$:

$$U \rightarrow U' = V \quad \text{if} \quad \tilde{\Delta}_\mu^2(x) = \frac{1}{a^6}\text{ReTr}(WW^\dagger - (UW^\dagger)^2) \geq \tilde{\delta}^2, \quad (5)$$

where $\tilde{\Delta}_\mu(x)$ is the dimensionful square of the lattice equations of motion. In the continuum limit (see [28])

$$\tilde{\Delta}_\mu^2(x) \rightarrow -2 \text{Tr}((D_\nu F_{\nu\mu}(x))^2); \quad (6)$$

hence we are locally requiring that the continuum equations of motion be satisfied to a degree specified by $\tilde{\delta}$. This corresponds to a constrained minimization problem. For $\tilde{\delta}=0$ cooling proceeds unrestricted, i.e. all links are updated at every iteration, whereas for large values of $\tilde{\delta}$ no changes are made at all and the configuration remains uncooled. Variation of $\tilde{\delta}$ then admits a smooth interpolation between these extreme cases.

In particular, for small $\tilde{\delta} > 0$ the configuration is changed only locally, where it is far from a classical solution, but freezes where it has approached a solution to a certain approximation specified by $\tilde{\delta}$ through Eq. (5). Since the equations of motion contain gradients of the fields, $\tilde{\delta}$ controls the energy of the fluctuations around classical solutions

and acts as a filter for short wavelengths. Hence cooling ends in a configuration slightly above the minimal action, the additional “action” being distributed smoothly over the lattice. We call this constrained variant of IC “restricted improved cooling” (RIC).

In this paper we have used a slightly different version of (5), specific for SU(2): we replace (5) by the condition:

$$U \rightarrow U' = V \quad \text{if} \quad \Delta_\mu(x)^2 = \frac{1}{a^6} \text{Tr}(1 - UV^\dagger) \geq \delta^2, \quad (7)$$

with V as in (4). In the continuum limit $\delta \propto \tilde{\delta}$ [28].

Lattice	$a^3\delta$	δ (fm ⁻³)	Saturation at sweep No.
$a=0.12$ fm	0.08	46.30	5
”	0.04	23.15	7
”	0.02	11.57	11
”	0.0085	4.92	22
”	0.005	2.89	40
$a=0.06$ fm	0.04/8	23.15	20
”	0.02/8	11.57	35
”	0.085/8	4.92	≈ 85
”	0.005/8	2.89	≈ 180

Table 2: *The number of cooling sweeps after which saturation is reached for RIC.*

Since RIC does not update links that are sufficiently close to a solution, it changes fewer links after every iteration until no further changes occur. On the MC configurations we define saturation to be reached when less than 1% of the links are updated in a sweep and end the cooling there². The number of cooling sweeps required to reach saturation is determined by δ . Some example values, for our SU(2) lattices, are given in Table 2. In Fig. 1 the fraction $\nu(n)$ of links updated per cooling iteration is shown for the $a = 0.06$ fm lattice at two different values of δ . The figure elucidates the difference between IC stopped at a certain number of sweeps and RIC. For the former, of course, ν is a step function whereas it is smeared out for RIC.

²We put this limit for practical reasons. We checked that it has little influence on the results: for very rough configurations (large δ) some narrow instantons may still shrink under cooling beyond this threshold; the effect is, however, at most 1–2% and disappears for smaller δ .

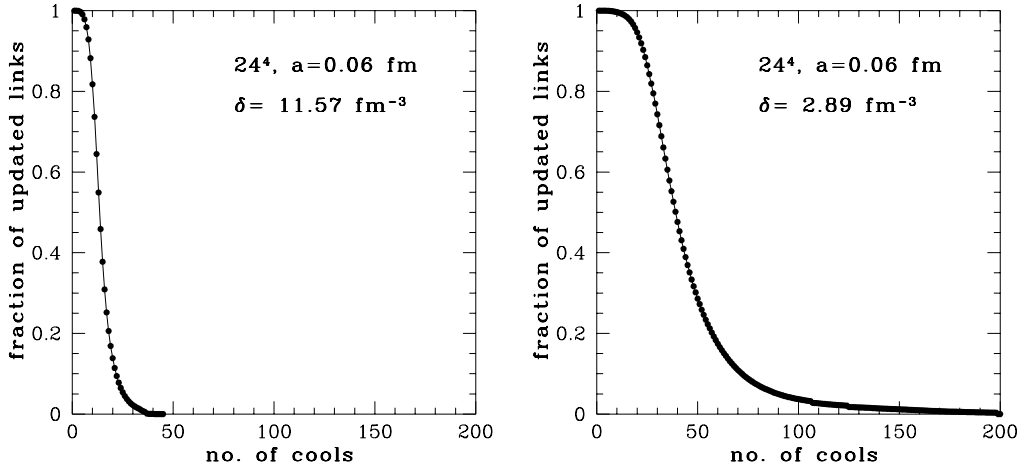


Figure 1: Fraction $\nu(n)$ of links updated per RIC iteration as a function of n for the $a = 0.06$ fm lattice.

3 Setting a scale for cooling

In order to establish a physical scale up to which cooling is effective, we study the behaviour of the string tension calculated on the cooled configurations. Such analyses have been carried out for other variants of cooling in [10, 22], indicating that the string tension is lost over increasingly large distances while cooling proceeds. In RIC, however, the amount of cooling is related locally to the equations of motion, which have a continuum limit. Hence, we expect to be able to find a scaling criterion for tuning the cooling parameter δ and thus define it directly in terms of a physical scale.

A standard way to calculate the string tension is to extract it from the exponential decay of the correlation function of spatial Polyakov loops $P^{(L)}$ of length L according to [29]

$$\sum_{\vec{x}} \langle P^{(L)}(x) P^{(L)\dagger}(0) \rangle \simeq e^{-aM_P^{(L)}t}, \quad aM_P(L) = a^2\sigma_L L, \quad a^2\sigma_\infty = a^2\sigma_L + \frac{\pi}{3L^2}. \quad (8)$$

In order to see when the asymptotic value $aM_P(L)$ is reached, one may look for plateaux in the effective mass on a given time slice,

$$aM(t) = -\frac{1}{L} \ln \frac{P^{(L)}(t+1)}{P^{(L)}(t)}. \quad (9)$$

For uncooled configurations, the signal is too noisy to extract the exponential fall-off. This problem is remedied by employing fuzzing techniques [1] to produce smeared operators with better overlaps onto the ground state. For the cooled configurations, this is usually not necessary as each cooling update includes the equivalent of one fuzzing step.

In Fig. 2 we show, for the $a = 0.12$ fm lattice in Table 1, the effective mass of the Polyakov loop for various numbers of cooling sweeps using IC or RIC ($\delta = 2.89$ fm⁻³).

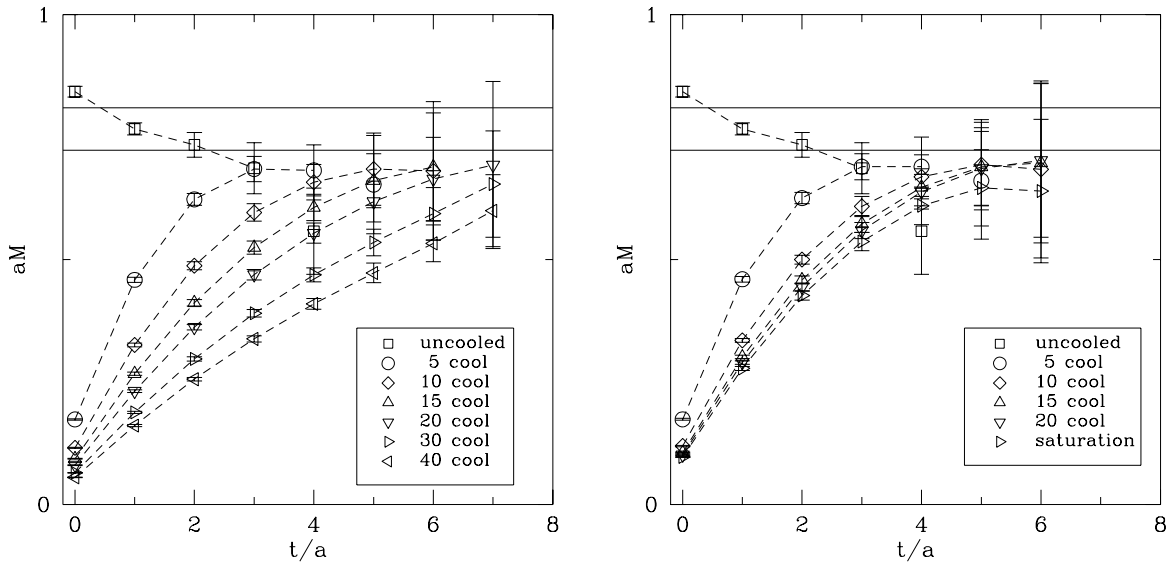


Figure 2: *Behaviour of effective masses of the Polyakov loop under cooling. Left: IC. Right: RIC with $\delta = 2.89 \text{ fm}^{-3}$. The dashed lines are to guide the eye. The horizontal line gives a string tension value (within the corresponding error band) as determined from [30].*

Since in this exploratory study we have rather poor statistics, we do not try to obtain a precise value for the string tension but are only interested in comparing the plateaux obtained from the uncooled and cooled correlation functions. For illustration we indicate in the figure the bandwidth of the value obtained from other data sets for the string tension [30]. The previously reported effect of a diminished string tension through cooling [10, 22] is clearly visible, and in both cases there is a “cooling radius” at which the effective masses merge with their counterparts from uncooled configurations, and beyond which the string tension is still unaffected. However, in the case of IC (as well as other cooling variants), this cooling radius moves to larger distances with the square root of the number of iterations [21]. As a consequence, the physical properties of the system are changed up to distances that are so large that beyond them any measurement of physical observables with reasonable statistical errors is practically impossible. In contrast, RIC saturates in the sense that no more changes take place above a certain number of iterations. The physical properties of the system beyond the cooling radius reached at saturation appear to remain intact.

Rather than by the number of iterations, the cooling radius for RIC is determined by the choice of the parameter δ , as displayed in Fig. 3. A larger choice for δ results in an “earlier” saturation, in the sense that links are left untouched when they represent a cruder approximation to the equations of motion, cf. Eq. (3). As elucidated in the figure, this results in a smaller cooling radius. The clear approach to saturation offers the possibility to fix the desired cooling radius *before* a simulation and eliminates the need to monitor

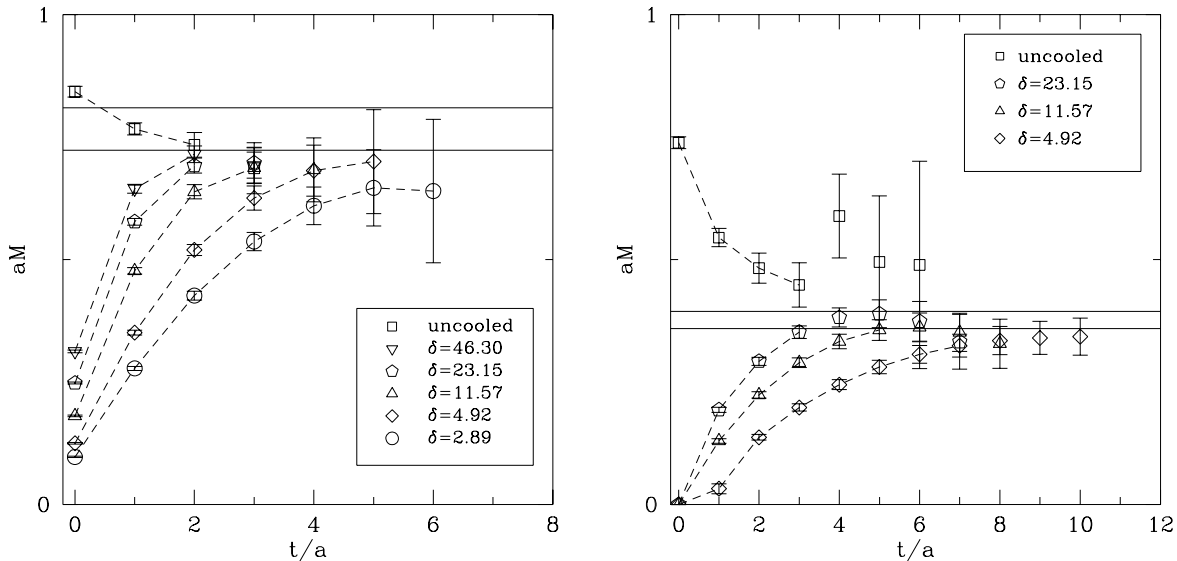


Figure 3: *The cooling radius of RIC as a function of δ . Left: $12^3 \times 36$, $\beta = 2.4$, $a = 0.12$ fm. Right: 24^4 , $\beta = 2.6$, $a = 0.06$ fm.*

the cooling process, which so far had to be stopped “by hand”, based on a subjective judgement on the trade off between smoothness of configurations and conservation of physical properties.

Furthermore, since the parameter δ is expected to have a continuum limit, it should be possible to establish a systematic mapping between the values of δ for a given lattice spacing and a physical length scale, up to which the smoothing process is active. This would permit a clean separation of physical scales into an ultraviolet sector, where smoothing is active, and an infrared sector, in which all physical properties are preserved. The naive expectation is that, close to the continuum limit, the dimensionful quantity δ should scale, cf. eq. (6). To check this behaviour we have repeated this study on the $a = 0.06$ fm lattice in Table 1, which halves the lattice spacing of the previous one while preserving the same 3-dimensional volume. The results for the effective mass on this lattice are presented in Fig. 3 (right). Despite the fact that the statistics is not very large, there is clear confirmation of this expectation. We extract the cooling radius $r(\delta)$ from Fig. 3 as the value of t at which the effective masses merge with the uncooled results and the string tension is recovered. A comparison of the data at fixed δ for the two values of a shows (at the level of precision of these data) good scaling properties and therefore allows us to estimate the physical cooling radius to be

$$r(\delta) \approx 0.8 \delta^{-1/3}. \quad (10)$$

Since the string tension gives the fundamental physical scale of the theory, we *conjecture* that *the cooling radius defined in this way is valid for all physical observables*, in the sense that all physical properties defined on scales larger than $r(\delta)$ can be measured

on configurations RI-cooled with δ . In the following we shall apply this conjecture to the observation of the topological structure.

4 Instantons and RIC

In order to provide a reliable extraction of the topological information from the MC configurations, there are two properties a smoothing algorithm should have:

(1) It should allow a clean separation between dislocations (small instantons at the scale of the cut off) and physical instantons. The former should be eliminated under smoothing, the latter should remain unaltered.

(2) Once we have fixed a physical distance below which smoothing is active, it should guarantee that the structure above it, among others instanton–anti-instanton pairs, remains unchanged.

Improved cooling was designed to achieve (1) and we shall prove below that RIC preserves this property. With respect to the string tension, RIC also satisfies requirement (2). As we shall see this is also the case for I-A pairs.

We present below the study of a set of prepared small instantons and I-A pairs that give an indication on the performance of RIC with respect to these two points. The reader interested only in the Monte Carlo results may skip this section and go directly to section 5.

4.1 Dislocations and RIC

The improved action in Eqs. (1), (2) was designed to minimize violations of scale invariance: it is almost independent of the instanton size ρ when the latter is above the threshold $\rho_0 \approx 2.3a$. Instantons with $\rho > \rho_0$ are practically left unchanged under cooling, irrespective of whether we use IC or RIC.

The situation is, however, quite different for small instantons with $\rho < \rho_0$. Under IC these instantons shrink and disappear through the lattice “holes”. Such small instantons are expected to deviate considerably from solutions to the equations of motion. To check this conjecture we have evaluated this deviation for a set of instantons with size below ρ_0 . We present on Fig. 4 (left) the dependence on ρ/a of the lattice dimensionless quantity:

$$\Delta_{\text{lat}}^{\text{peak}} = \frac{a^3}{4} \sum_{\mu} \Delta_{\mu}(x^0), \quad (11)$$

with $\Delta_{\mu}(x)$ from Eq. (7), evaluated on top of the instanton. As expected, for $\rho < \rho_0$ the deviation from a solution increases in a rather steep way with decreasing instanton size. RIC limits $\Delta_{\mu}(x) \leq \delta, \forall x$; in the figure we indicate by horizontal dotted lines the

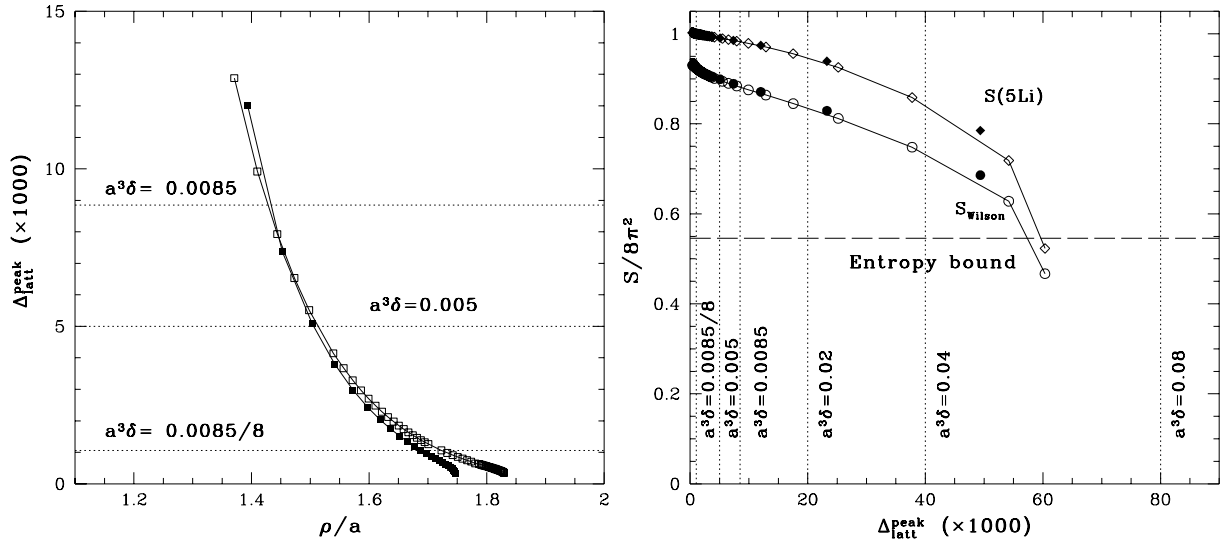


Figure 4: *Left: Dimensionless deviation from a solution of the equations of motion: $\Delta_{\text{latt}}^{\text{peak}}$ – see Eq. (11) – as a function of the instanton size in lattice units. Right: Action of small instantons as a function of $\Delta_{\text{latt}}^{\text{peak}}$. The horizontal dashed line indicates the entropy bound: instantons with S_{Wilson} below this line should be considered as dislocations [31]. On the left (right) figure the horizontal (vertical) dotted lines show the values of $a^3\delta$ used in our RIC simulations. Open (filled) symbols correspond to the $a = 0.12$ (0.06) fm lattice.*

values of $a^3\delta$ used in our RIC simulations. Instantons with $\Delta_{\text{lat}}^{\text{peak}}$ above each line will be destroyed under RIC with the corresponding δ . We may as well say that instantons with size below $\rho_0^{\text{RIC}}(a^3\delta)$ will shrink and disappear under RIC with δ , where $\rho_0^{\text{RIC}}(a^3\delta)$ is given by the intersections of the curves on Fig. 4 (left) with the horizontal lines.

We present on the figure data for both $a = 0.12$ and 0.06 fm. It is important to note that we are plotting the deviation from a solution evaluated in lattice (not physical) units. The rather weak dependence on a for $\rho/a < 2$ indicates that for instantons close to the lattice spacing the scaling law given by Eq. (6) does not hold, and the deviation from a solution is fixed solely in terms of the size in lattice units, i.e. ρ/a .

To summarize, setting δ allows to fix a threshold $\rho_0^{\text{RIC}}(a^3\delta)$ on the size of the instantons that will be preserved under RIC. $\delta = 0$ corresponds to the IC threshold $\rho_0 \equiv \rho_0^{\text{RIC}}(\delta = 0) \approx 2.3a$. For $\delta \neq 0$, the dislocation threshold (in lattice units) is smaller for larger lattice spacing.

As pointed out before, the existence of this small instanton threshold is important to avoid the presence of dislocations after cooling. A semi-classical argument due to Pugh and Teper [31] indicates that lattice instantons with action below the so-called entropy bound, $S_{\text{lattice}}(\rho) \leq 48\pi^2/11$, dominate the path integral in the continuum limit and give rise to the lattice artefacts known as dislocations; for details of the argument, see [31]. Since we have generated the MC configurations with the Wilson action (S_{Wilson}) this is

the relevant quantity to characterize small instantons as dislocations. In Fig. 4 (right) we show the improved action as well as S_{Wilson} for the instantons in Fig. 4 (left). According to the above, instantons with S_{Wilson} below the entropy bound (indicated on the figure by the dashed horizontal line) should be considered as dislocations. As can be seen from the figure the deviation from a solution of the equations of motion for such configurations is quite large. It is then obvious that they can be eliminated by putting a threshold on the maximally allowed deviation and this is precisely what RIC does. We indicate in the figure by dotted vertical lines the values of $a^3\delta$ used in our RIC simulations. It seems that topological lattice artefacts are under control with RIC as long as we keep $a^3\delta < 0.04$.

4.2 I-A pairs and RIC.

One of the motivations for RIC was to introduce a physical scale above which the physical information concerning I-A pairs remained unaltered. Both on the lattice and in the continuum, these configurations are not solutions of the classical equations of motion, unless the instanton and anti-instanton are infinitely separated from each other. Since ordinary cooling is an unconstrained local minimization of the action, when cooled with it the I and A annihilate and decay into the trivial vacuum. The information concerning I-A pairs extracted from ordinary cooling is hence distorted in an uncontrolled way. RIC cooling, on the contrary, will leave unchanged those pairs for which the deviation from a solution remains everywhere smaller than δ . The expectation is that this provides a means to fix a physical scale above which the information concerning pairs is unchanged.

To test this hypothesis we have analysed a prepared set of I-A pairs (similar studies for other variants of cooling have been performed in [15]). As in [15] we create a pair by putting together a $Q = 1$ instanton and, at a distance d_{IA} along the time direction, the anti-instanton obtained from it by time reversal. This configuration is I-cooled and its evolution is studied under cooling. We have monitored in particular the change of the deviation from a solution as evaluated at the instanton centre (x^0) and at the mid-point between I and A (x^m):

$$\Delta^{0,m} = \frac{1}{3} \sum_{i=1}^3 \Delta_i(x), \text{ with } x = x^0, x^m, \quad (12)$$

where $\Delta_i(x)$ is given by Eq. (7) (the deviation measured on links along the separation axis is much smaller, therefore we did not include it in the estimate of $\Delta^{0,m}$). The results are presented in Fig. 5 (left). This figure should be interpreted as providing a series of I-A configurations labelled by the number of IC sweeps. As expected, with proceeding IC $\Delta^{0,m}$ increases (the configuration gets distorted away from a solution) until it decays into a trivial one; after that we can no longer recognize I and A as peaks in the energy density,

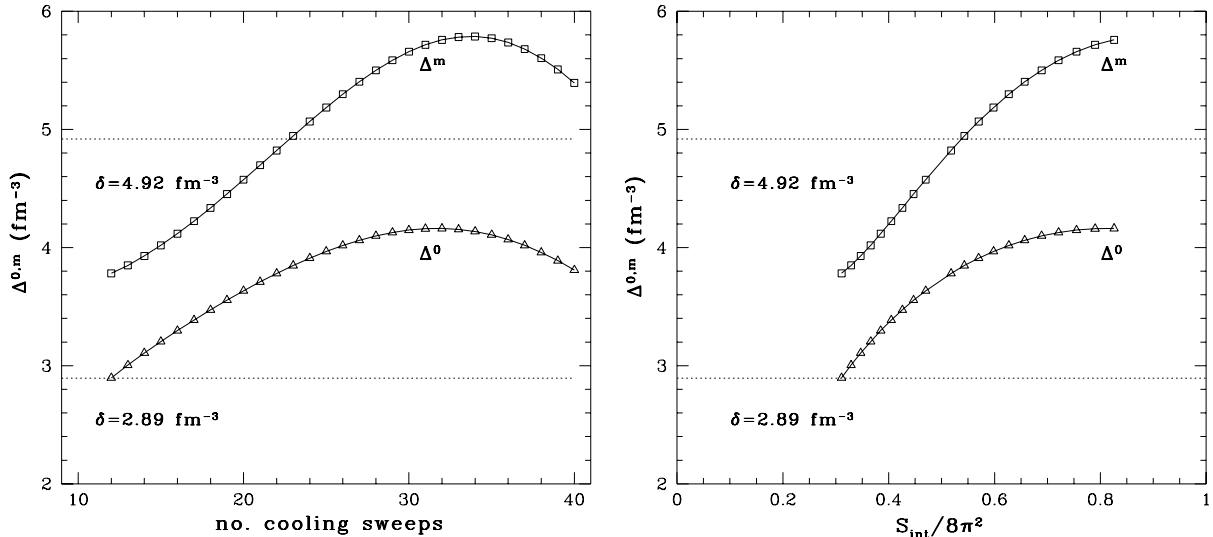


Figure 5: *Left: Evolution of the deviation from a solution of the equations of motion $\Delta^{0,m}$ – see Eq. (12) – under IC as a function of the number of cooling sweeps. Right: $\Delta^{0,m}$ vs S_{int}^{IA} – see Eq. (13). The results are obtained on the $a = 0.12$ fm lattice. The horizontal dotted lines show the values of δ used in our simulations. Pairs for which $\Delta_{\mu}(x)$ is below the line for all x are preserved under RIC with δ .*

the configuration approaches the trivial vacuum and $\Delta^{0,m}$ decreases again. This picture changes under RIC. We have plotted in the figure horizontal dotted lines corresponding to the values of δ used in our simulations. Whenever a configuration satisfies $\Delta_{\mu}(x) \leq \delta$ everywhere, in particular at x^0 and x^m , it will be left untouched by RIC, i.e. the pair will be preserved and will not annihilate under RIC with δ . Pairs with $\Delta^{0,m}$ above the line will, however, be destroyed.

Our objective is now to fix which pairs are preserved, using a physical length scale, since this may allow us to relate their effects to the physical quantities characterized by that scale. As already mentioned, since I-A pairs are continuously connected with the trivial vacuum, there is an ambiguity (in the continuum) in distinguishing a pair from a trivial fluctuation. The threshold separating the two is usually rather arbitrary and set “by hand”. One possibility is to do it through the value of the interaction between I and A,

$$S_{\text{int}}^{IA} = 16\pi^2 - S^{IA}. \quad (13)$$

It seems only justified to speak of an I-A pair instead of a fluctuation if S_{int}^{IA} remains considerably smaller than the action of a “non-interacting” pair: $16\pi^2$. We can thus parametrize I-A pairs in terms of how small S_{int}^{IA} is, and use it as a threshold for which pairs will be considered as physical. We have monitored S_{int}^{IA} for the pairs in Fig. 5 (left) and the results are presented in Fig. 5 (right). Whenever we are able to still recognize the I and A there is a one to one correspondence between the distance to a solution (notice

$\Delta^{0,m}$ is a dimensionful quantity) and $S_{\text{int}}^{\text{IA}}$.

If we parametrize I-A pairs through how small $S_{\text{int}}^{\text{IA}}$ is, it is clear that setting δ is equivalent to putting a cut on which pairs will be considered as physical and which will be thrown away according to the value set for the maximal $S_{\text{int}}^{\text{IA}}$. It is in this sense that RIC implements the valley method constraint, since it amounts to a local constrained minimization of the action that prevents the interaction to act along the valley between I and A, if such an interaction is smaller than the chosen $S_{\text{int}}^{\text{IA}}$.

5 Monte Carlo results

5.1 Topological susceptibility from RIC

Lattice	$a^3\delta$	$\delta \text{ fm}^{-3}$	$^4\sqrt{\chi} \text{ MeV}$	$\langle Q^2 \rangle$	$\langle S \rangle / 8\pi^2$	$\langle Q \rangle$
$a=0.12 \text{ fm}$	no cooling		172(2)	7.4(3)	10634(1)	2.16(5)
"	0.08	46.30	190(3)	10.9(7)	443.9(2)	2.6(1)
"	0.04	23.15	194(4)	11.9(9)	210.0(2)	2.8(1)
"	0.02	11.57	199(3)	13.2(8)	109.7(2)	2.93(9)
"	0.0085	4.92	198(2)	13.0(6)	51.7(1)	2.91(6)
"	0.005	2.89	197(3)	12.6(8)	33.3(3)	2.85(8)
"	IC nc=20		199(2)	13.1(6)	25.2(2)	2.91(8)
"	IC nc=40		197(2)	12.6(7)	15.4(2)	2.86(8)
$a=0.06 \text{ fm}$	no cooling		297(4)	22(1)	50482(4)	3.7(1)
"	0.04/8	23.15	203(7)	4.7(6)	80.4(2)	1.7(1)
"	0.02/8	11.57	203(7)	4.8(5)	40.3(2)	1.7(1)
"	0.0085/8	4.92	210(7)	5.4(5)	18.8(2)	1.8(1)
"	IC nc=20		205(7)	4.9(7)	30.8(2)	1.7(1)
"	IC nc=50		205(7)	5.0(7)	12.9(2)	1.7(1)

Table 3: *Topological susceptibility χ , average charge squared $\langle Q^2 \rangle$, action $\langle S \rangle / 8\pi^2$ and absolute value of the topological charge $\langle |Q| \rangle$, from IC and RIC.*

The results for the topological susceptibility are presented in Table 3 and Fig. 6. For comparison we also include in the table and the figure the results for the topological susceptibility extracted directly from the MC configurations (without smoothing). As expected, the raw Monte Carlo data indicate strong deviations from scaling which, comparing to the

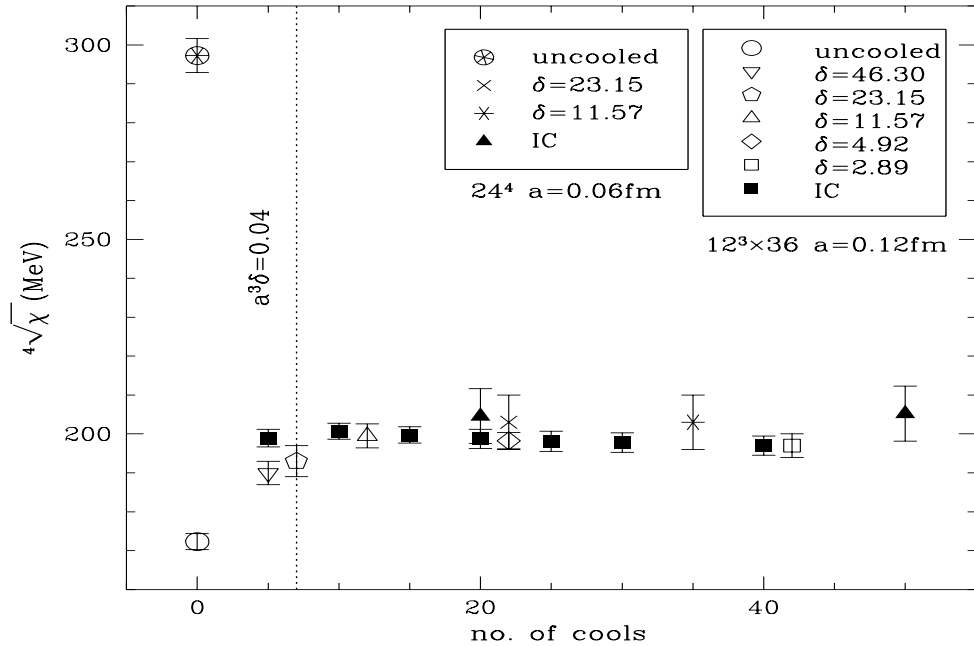


Figure 6: *Topological susceptibility with IC and RIC. The results from RIC are plotted at the number of cooling sweeps corresponding to saturation – see Table 2.*

IC results, are particularly severe for the finer lattice ³.

The expectation expressed in section 4.2 that changing $a^3\delta$ allows to change the threshold on small instantons, and hence on dislocations, is corroborated by the MC data. The result on the $a = 0.12$ fm lattice at $a^3\delta = 0.08$ is clearly affected by dislocations, as seen in the tendency to approach the uncooled results. According to this observation and in view of the strong scaling violations of the uncooled data, it seems quite dangerous to extract the value of the topological susceptibility by extrapolating to zero smoothing. Generally, a minimal amount of smoothing may be indispensable to obtain a physically meaningful value for the susceptibility; see also [32].

By contrast, in the “safe” region ($a^3\delta < 0.04$) we observe good agreement between the different results, including good scaling behaviour when comparing the $a = 0.12$ and 0.06 fm lattices. This is an indication that most of the relevant physical instantons have been correctly taken into account and have sizes above the small instanton thresholds $\rho_0^{RIC}(a^3\delta < 0.04)$.

The results agree well with the Witten-Veneziano formula and with results obtained previously by us using IC [11, 12], as well as by other groups using different methods [2, 14, 15]. Differences with the results in [3] appear only for the largest β value and amount to about 10% of the value of χ .

³This is to be expected for MC configurations generated with the Wilson action, since the simple semi-classical argument quoted above [31] indicates that the contribution of dislocations to the Wilson action partition function diverges in the continuum limit.

5.2 Instanton ensemble from RIC

A first impression of the effect of RIC is already given by the average value of the action presented in Table 3. Assuming that after some smoothing the action is mostly saturated by $|Q| = 1$ instantons, the average action gives an estimate of the total number of instantons. It is clear that, under the above assumption, large δ keeps more instantons, i.e. less pairs are annihilated. Moreover the scaling behaviour of δ is confirmed within at most 10% difference by comparing the average value of the action per unit volume between the $a = 0.12$ fm lattice at $\delta = 23.15, 11.57, 4.92 \text{ fm}^{-3}$: $S/V = 16.28(2), 8.78(2), 4.57(1) \text{ fm}^{-4}$; and the corresponding values on the $a = 0.06$ fm lattice: $S/V = 18.49(4), 9.27(4), 4.32(4) \text{ fm}^{-4}$.

To associate the action with an instanton ensemble one has to extract in some way the instanton content of the configurations. This is a difficult task due to several reasons:

(i) as pointed out before, there is an ambiguity in distinguishing between an I-A pair and a trivial fluctuation;

(ii) this ambiguity is enhanced if the ensemble is dense, as seems to be the case, since then the objects in the ensemble are strongly overlapping.

This last point sheds quite some doubts on the reliability and usefulness of the instanton parametrization, unless one can justify the introduction of some physical criterion to select the relevant pairs for the process under consideration. In particular, the results obtained for instance for the size distribution seem to be quite dependent on the particular method used to smooth and analyse the configurations (see [19]).

Our particular way of extracting the instanton information out of the configurations relies on two assumptions: (1) instantons should appear as local self-dual peaks in the action and charge density; (2) only pairs with $S_{\text{int}}^{\text{IA}}$ considerably smaller than $16\pi^2$ should be considered as such. Hence we approximate the action and charge density by a superposition of self-dual non-interacting instantons and anti-instantons parametrized through the 1-instanton BPST ansatz (further details on the procedure are provided in the Appendix). We can measure the departure of the real action and charge density from the above non-interacting ansatz through the quantities

$$\varepsilon_q = \sqrt{\frac{\int d^4x |q(x) - q_{\text{fit}}(x)|^2}{\int d^4x |q(x)|^2}} \quad (14)$$

and ε_s , defined as ε_q with the replacement $q \rightarrow s$. In previous work we have adopted the prescription of performing a minimal amount of cooling such that the deviations from the ansatz described above were at most 0.3. Under this restriction, and using IC, we observed:

(i) for the minimal level of smoothing, a rather dense ensemble with a number of

instantons by about a factor of 2 larger than the dilute gas prediction $\langle N \rangle = \langle Q^2 \rangle$, with N the number of instantons plus anti-instantons;

(ii) a size distribution peaked at about 0.4 fm and rather stable under further cooling (a much smaller average size of ~ 0.2 fm has been reported in [3, 16], extracted from smeared configurations and under extrapolation to no-smearing; see 5.2.2 for further discussion);

(iii) a rather homogeneous distribution of I and A, which seem to be randomly distributed over the lattice.

For the largest values of δ in our RIC analysis we will present results corresponding to values of $\varepsilon_{s,q}$ up to 0.6, where only a small part of the action and charge density is correctly described by our instanton ansatz. These results should be taken with care, since they correspond to rather dense ensembles and, as mentioned above, in such case there is a significant ambiguity in the extraction of the instanton content. The aim in the present work is to study the results obtained by our instanton finder as a function of δ in RIC.

5.2.1 Results

Now we turn to the analysis of the Monte Carlo configurations. Results are presented in Table 4.

a	δ (fm ⁻³)	$r(\delta)$	$\langle N/V \rangle$	$\langle O_{II} \rangle$	$\langle O_{IA} \rangle$	$\langle d_{II} \rangle$	$\langle d_{IA} \rangle$	ε_q (ε_s)	$\langle \rho \rangle$
0.12	23.15	0.24(5)	14.86(7)	0.95	1.28	0.39	0.28	0.75(0.55)	0.38
"	11.57	0.35(5)	8.72(2)	0.86	1.08	0.46	0.36	0.60(0.45)	0.40
"	4.92	0.50(5)	4.21(2)	0.79	0.88	0.54	0.49	0.45(0.35)	0.42
"	2.89	0.60(5)	2.70(3)	0.76	0.79	0.59	0.58	0.35(0.30)	0.44
"	IC(20)		2.06(2)	0.70	0.72	0.61	0.61	0.30(0.30)	0.42
0.06	23.15	0.27(3)	18.7(1)	0.93	1.20	0.40	0.30	0.60(0.45)	0.35
"	11.57	0.35(3)	9.6(1)	0.84	1.02	0.48	0.39	0.45(0.40)	0.38
"	4.92	0.55(3)	4.35(6)	0.77	0.85	0.57	0.53	0.25(0.25)	0.40
"	IC(50)		2.96(5)	0.68	0.71	0.59	0.57	0.25(0.25)	0.37

Table 4: *Cooling results for IC at 20 and 50 cooling sweeps and for RIC at various δ . The lattice spacing (a), the cooling radius ($r(\delta)$), distances and sizes are given in fm. The density $\langle N/V \rangle$ is in fm⁻⁴. The errors are statistical, when they are not explicitly quoted they amount to 1 or less in the last indicated digit.*

We are mostly interested in studying the performance of RIC with respect to I-A pairs. First we observe that the density of instantons (N/V in Table 4) increases with δ . This corroborates the finding that less I-A annihilation takes place for large δ . Moreover the

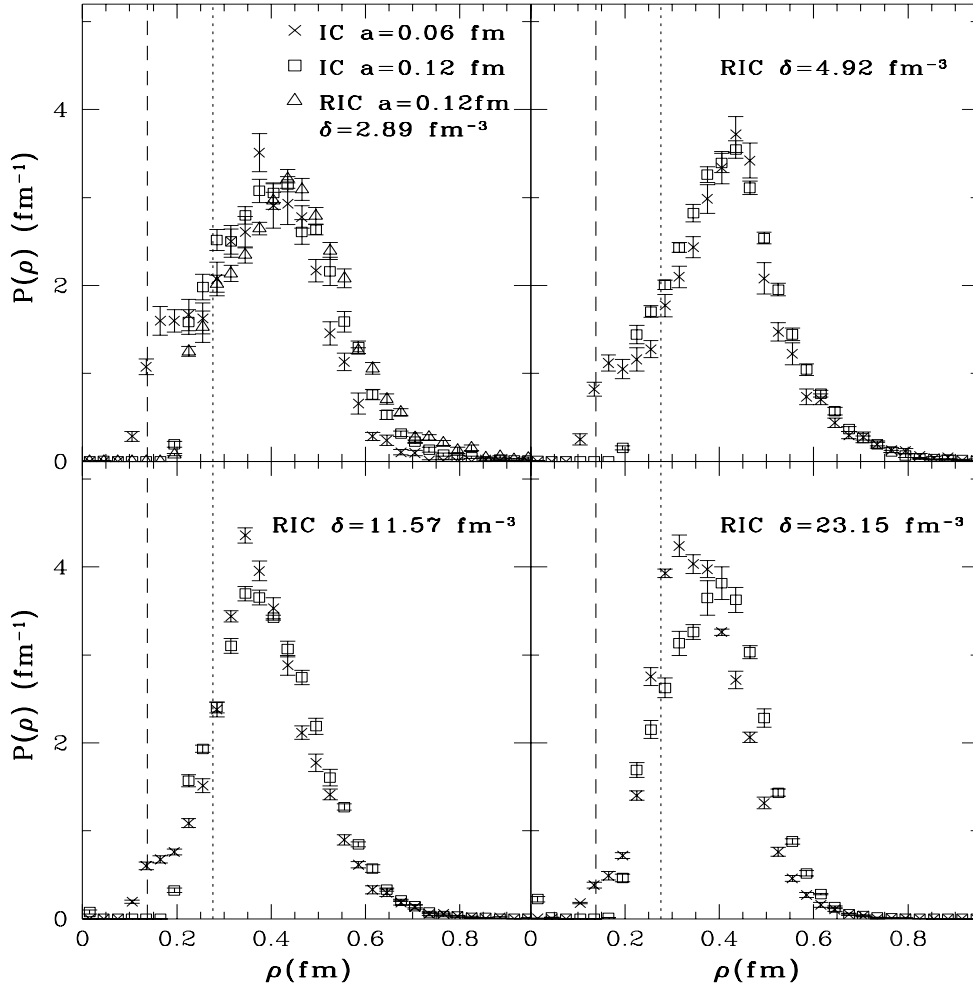


Figure 7: Size distributions on the $a = 0.12 \text{ fm}$ lattice (squares, triangles) and $a = 0.06 \text{ fm}$ lattice (crosses). The vertical dotted (dashed) lines indicate the location of the IC dislocation threshold $\rho_0 = 2.3a$ on the $a = 0.12$ ($a = 0.06$) fm lattice.

density scales correctly (up to at most 10% (20% for the largest δ) difference) by comparing the results for the two lattice spacings at fixed δ .

We define pairs in this ensemble by assigning to each instanton the anti-instanton that has maximal overlap O_{IA} with it; O_{IA} is defined as:

$$O_{IA} = \frac{\rho_I + \rho_A}{2d_{IA}}, \quad (15)$$

where $\rho_{I,A}$ are the sizes and d_{IA} the distance between I and A. The results for the average overlap and separation are given in Table 4. As expected, large δ preserves stronger overlapping pairs. Notice the good agreement between the pair separation d_{IA} and the cooling radius $r(\delta)$, Eq. (10), a clear indication that smoothing has been active in removing pairs with a separation smaller than the cooling radius. As we will further discuss below, this also indicates that there does not seem to be an intrinsic scale for I-A separation apart from the one given by $r(\delta)$ itself.

For comparison we also present in Table 4 the overlap and separation between maximally overlapping objects of the same charge. Note that for large δ , i.e. denser ensemble, objects with opposite charges are closer on average than objects with equal charges. However, in our earlier IC analysis [12], which roughly corresponds to RIC at small δ , we observed a homogeneous distribution of I and A over the lattice. The difference can be understood by noticing that pairs with strong overlap will be removed faster during cooling, and have probably been eliminated at the stage of smoothing provided by IC. Since the action of an I-A pair decreases as the overlap increases and is smaller than that of an I-I or an A-A pair, it is indeed energetically favourable that I-A pairs overlap more.

In Fig. 7 we present the instanton size distribution as a function of δ , Table 4 provides the average instanton size $\langle\rho\rangle$. Since IC and RIC converge to scale-invariant instanton configurations, the instanton sizes, in contrast to other physical quantities, should not change when the cooling radius increases beyond them (up to modifications that would be induced by I-A annihilation and possible dressing of the instantons by fluctuations). This is certainly the case for the results obtained with IC above the minimal smoothing level (see [12]) and also for RIC with small δ (i.e. density of instantons below 4 fm^{-4}). Note, however, that now we go to much denser and rougher ensembles. At these densities the stability of the size distribution is not as apparent, both the average size and the shape of the distribution weakly depend on the smoothing level. The increase in the close pair population seems to lead to a certain shift in the average size, both by spoiling the size estimate and by re-weighting the size distribution⁴. It is difficult to evaluate which of these two effects dominates, cf. the debate about this problem in the literature (for reviews, see [18, 19]). According to [3] smoothing the configurations induces a modification of the size and the correct one should be obtained by linear extrapolation to zero smoothing levels (for SU(3) this seems to give rough agreement between the results from different smoothing techniques [19]). Our attitude is not to trust the size determination corresponding to large densities (small cooling radius), since, as we have discussed, it is difficult in such cases to obtain a reliable description of the action and charge density in terms of instantons (the deviations amount to 0.6 (0.5) of the total charge (action)).

This problem cannot be easily solved and is indeed farther reaching, since it is related to the general question of whether there exists an effective I-A density relevant for a given physical effect. The numerical agreement between the cooling radius and the I-A separation – see Table 4 – suggests that the latter is determined by the former, i.e. there appears to be no intrinsic scale for I-A separation independent of the one set by the smoothing scale itself.

⁴Note that the size distributions of Fig. 7 are normalized, while describing instanton populations varying by a factor up to 10.

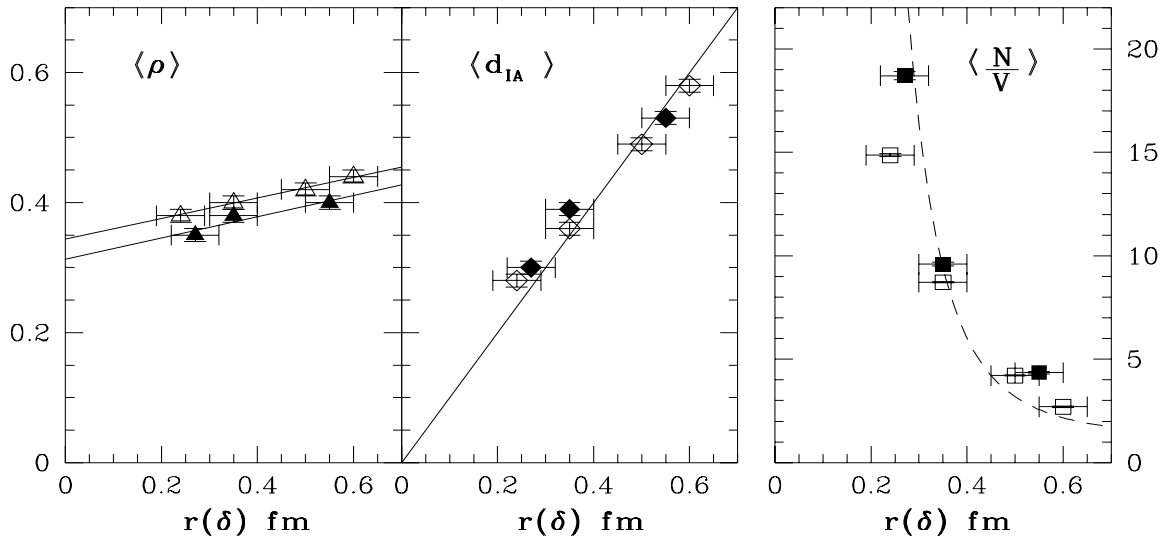


Figure 8: Dependence of the average size (triangles), the I - A average distance (diamonds) and the instanton density (squares) on the cooling radius r . The dashed curve fits the density data to $\langle N/V \rangle = \langle N/V \rangle_{\text{asymptotic}} + C/r^4$. Open (filled) symbols correspond to the $a = 0.12$ (0.06) fm lattice.

In order to elaborate on this, we consider again the instanton properties as a function of the cooling radius. It is apparent from Fig. 7 and Fig. 8 that the dependence of the average size upon $r(\delta)$ is rather weak, even at small $r(\delta)$ (large δ). This seems to indicate the existence of a non-vanishing, dominant instanton size even at cooling radius zero. However, Fig. 8 also shows the different behaviour of the density $\langle N/V \rangle$ and of the pair separation $\langle d_{IA} \rangle$. A simple extrapolation of the data to zero cooling radius is compatible with a diverging density and a vanishing I-A distance. This is in accord with the fact that there is no principal distinction between a trivial fluctuation and an instanton-anti-instanton pair, apart from the somewhat arbitrary criterion given in terms of $S_{\text{int}}^{\text{IA}}$. This supports the observation made above that there appears to be no average I-A separation or instanton density that could be defined independently of the smoothing scale (at least up to the scales we have probed). Thus, speaking of an instanton ensemble seems to be possible only in the context of smoothing and by providing a specific smoothing scale. If this is indeed the case, a criterion for selecting “physically relevant” pairs may only come from considering the relevant scale of the phenomena to which we can expect these pairs to contribute.

6 Conclusions and Outlook

By fixing the amount of cooling with the help of a *cooling radius* ($r(\delta)$) above which physical observables such as the string tension remain untouched, restricted improved cooling

provides a *smoothing scale* for treating MC configurations. Because of its connection with the equations of motion this scale appears as a continuum length scale, which can be systematically determined from the measurement of one physical quantity. Starting from the rough, UV-dominated field configurations (cooling radius $r = 0$), RIC with increasing r acts as a “low-pass filter” by smoothing out wavelengths smaller than r and producing configurations on which correlation functions at distances beyond r retain the physics of the larger wavelengths. The conjecture that the cooling radius $r(\delta)$ provides a universal smoothing scale seems well supported by our analysis.

The observation of topological structure itself poses a difficult problem. The topological susceptibility appears to be quantitatively under control, but the more detailed topological structure raises many questions. Firstly, for very small cooling radius the observed structure is very dense and only poorly described in semi-classical terms. Secondly, we find that cooling uncovers topological structure on scales close to the cooling radius. While the instanton size distributions are rather stable under variations of the smoothing scale, the instanton density and the mean separation of instanton–anti-instanton pairs appear to be determined by it. Decreasing the smoothing scale, this structure thus becomes denser until it continuously disappears into the UV fluctuations. Hence, for these quantities, an extrapolation to no smoothing does not lead to meaningful results. On the other hand, it appears to be quite arbitrary to choose from the observed structure a “physical” sub-ensemble by fixing a finite smoothing scale. It may well be that the characteristic length scale of the phenomena under scrutiny has to be taken into account when establishing the criteria for finding an “effective” relevant structure that contributes to these phenomena. Here RIC may provide a useful tool, since it introduces a smoothing radius as a continuum length scale, which can be systematically varied in the analysis.

Further studies should provide improved statistics for the precise determination of the cooling radius and the other properties of RIC, but also a better theoretical understanding of these questions.

Acknowledgements

It is a pleasure to thank Ferenc Niedermayer for suggesting the modification of cooling that initiated this study, and for discussions. We also thank Pierre van Baal for a critical reading of the manuscript and discussions. Part of this work has been performed while M.G.P. and I.O.S. were members of the ISKOS workshop at ZiF, Bielefeld. Partial support from the European Network “Finite Temperature Phase Transitions in Particle Physics” and from DFG is gratefully acknowledged. M.G.P. would also like to acknowledge support from CICYT and hospitality at CERN’s Theory Division while part of this work was being

performed.

Appendix

We provide a few details about the way we perform the extraction of the instanton content from the configurations (a more detailed description of the method will be presented elsewhere).

As already mentioned in section 5, our instanton identifier relies on the following assumptions:

1. Instantons are self-dual objects with energy density localized in space and time. Self-duality imposes, in particular, that the localization of the peaks should be the same in the electric and magnetic parts of the action density and also in the charge density (for details on how we imposed the cut from self-duality, see [12]).
2. We approximate the action and charge density by a superposition of self-dual non-interacting instantons and anti-instantons parametrized through the analytic expression for the 1-instanton action and charge density:

$$s_i(x) = \frac{48}{(\rho^i)^4} \left[1 + \sum_{\mu=1}^4 \left(\frac{x_\mu - c_\mu^i}{\rho^i} \right)^2 \right]^{-4}, \quad (16)$$

$$s_{\text{fit}}(x) = \sum_{i=1,N} s_i(x); \quad q_{\text{fit}}(x) = \frac{1}{8\pi^2} \sum_{i=1,N} n_i s_i(x), \quad (17)$$

with $N = N_I + N_A$ the number of instantons plus anti-instantons, ρ^i and c_μ^i respectively the size and location of the i th (anti)instanton and $n_i = 1$ for an instanton, $n_i = -1$ for an anti-instanton⁵.

The departure of the real action and charge from the above formula is measured through the quantities $\varepsilon_{q,s}$ given in Eq. (14). For the analysis in this paper we have supplemented the one performed in [12] with a further restriction: every time an instanton candidate is located, it is counted only if, by adding it to s_{fit} and q_{fit} , $\varepsilon_{s,q}$ simultaneously decrease. Once the instanton has been accepted, its contribution ($s_i(x)$) is subtracted from the total density before proceeding to analyse the next instanton candidate. Note that this procedure assumes that all self-dual objects in the ensemble can be described in terms of a superposition of instantons following the BPST ansatz (other possible self-dual objects, which are not well parametrized by this ansatz, would be discarded by our $\varepsilon_{s,q}$

⁵ To account for periodicity effects we add to the energy density of each instanton the eight closest replicas, obtained by displacing (16) by a torus period in one of the four directions.

cuts). A small value of $\varepsilon_{s,q}$ is, hence, a signal that most of the structure present in the ensemble is well described in these terms.

As an example of the kind of results we expect, let us consider the I-A pairs in Fig. 5, where ε_s (ε_q) varies from about 0.1 (0.05), for the pair with smallest $S_{\text{int}}^{\text{IA}}$ in the figure, to 0.32 (0.18), for the one with largest $S_{\text{int}}^{\text{IA}}$. Beyond the latter, our instanton finder fails to identify I and A any longer. In the same way, for the small instantons in Fig. 4, ε_s (ε_q) goes from 0.05 (0.15) for the largest one in the figure to 0.06 (0.86) for the smallest one. Again beyond that point our finder no longer sees an instanton at this location.

References

- [1] M. Albanese et al., Phys. Lett. B192 (1987) 163; Phys. Lett. B197 (1987) 400.
M. Teper, Phys. Lett. B183 (1987) 345; Phys. Lett. B185 (1987) 121.
- [2] C. Christou, A. Di Giacomo, H. Panagopoulos and E. Vicari, Phys. Rev. D53 (1996) 2619; B. Alles, M. D’Elia and A. Di Giacomo, Nucl. Phys. B494 (1997) 281; Nucl. Phys. Proc. Suppl. 53 (1997) 541; Phys. Lett. B412 (1997) 119.
- [3] T. De Grand, A. Hasenfratz and T. G. Kovacs, Nucl. Phys. B520 (1998) 301. A. Hasenfratz and C. Nieter, hep-lat/9806026; hep-lat/9810067.
- [4] P. de Forcrand and J. E. Hetrick, Nucl. Phys. Proc. Suppl. 63 (1998) 838.
- [5] B. Berg, Phys. Lett. B104 (1981) 475; Y. Iwasaki and T. Yoshie, Phys. Lett. B131 (1983) 159; S. Itoh, Y. Iwasaki and T. Yoshie, Phys. Lett. B147 (1984) 141; M. Teper, Phys. Lett. B162 (1985) 357; J. Hoek, M. Teper and J. Waterhouse, Nucl. Phys. B288 (1987) 889.
- [6] E. M. Ilgenfritz, M. L. Laursen, G. Schierholz, M. Muller-Preussker, H. Schiller, Nucl. Phys. B268 (1986) 693.
- [7] M. I. Polikarpov and A. I. Veselov, Nucl. Phys. B297 (1988) 34.
- [8] C. Michael and P. S. Spencer, Phys. Rev. D52 (1995) 4691.
- [9] M. C. Chu, J. M. Grandy, S. Huang and J. W. Negele, Phys. Rev. D49 (1994) 6039.
- [10] A. González-Arroyo, P. Martínez and A. Montero, Phys. Lett. B359 (1995) 159;
A. González-Arroyo and A. Montero, Nucl. Phys. Proc. Suppl. 47 (1996) 294; Phys. Lett. B387 (1996) 823; Nucl. Phys. Proc. Suppl. 53 (1997) 596.

- [11] P. de Forcrand, M. García Pérez and I. O. Stamatescu, Nucl. Phys. Proc. Suppl. 47 (1996) 777; Nucl. Phys. Proc. Suppl. 53 (1997) 557.
- [12] P. de Forcrand, M. García Pérez and I. O. Stamatescu, Nucl. Phys. B499 (1997) 409.
- [13] P. de Forcrand, M. García Pérez, J. E. Hetrick and I. O. Stamatescu, Nucl. Phys. Proc. Suppl. 63 (1998) 549, hep-lat/9802017.
- [14] M. Teper, “Physics from the lattice: Glueballs in QCD: Topology: SU(N) for all N” in *Cambridge 1997, Confinement, duality, and nonperturbative aspects of QCD*, p. 43 (hep-lat/9711011); D. A. Smith and M. Teper, Phys. Rev. D58 (1998) 014505.
- [15] A. Montero, “ Confinamiento y configuraciones clásicas”, PhD thesis (1998), Universidad Autónoma de Madrid.
- [16] T. DeGrand, A. Hasenfratz and D. Zhu, Nucl. Phys. B475 (1996) 321; Nucl. Phys. B478 (1996) 349. T. DeGrand, A. Hasenfratz and T. G. Kovacs, Nucl. Phys. B505 (1997) 417.
- [17] M. Feurstein, E. M. Ilgenfritz, M. Müller-Preussker and S. Thurner, Nucl. Phys. B511 (1998) 421. E. M. Ilgenfritz et al., Nucl. Phys. Proc. Suppl. 63 (1998) 480; E. M. Ilgenfritz et al., Phys. Rev. D58 (1998) 094502; E. M. Ilgenfritz and S. Thurner, hep-lat/9810010.
- [18] P. van Baal, Nucl. Phys. Proc. Suppl. 63 (1998) 126.
- [19] J. W. Negele, hep-lat/9810053.
- [20] M. Teper, Nucl. Phys. B411 (1994) 855.
- [21] A. Di Giacomo, E. Meggiolaro and H. Panagopoulos, Nucl. Phys. Proc. Suppl. 54A (1997) 343.
- [22] M. Campostrini, A. Di Giacomo, M. Maggiore, H. Panagopoulos and E. Vicari, Phys. Lett. B225 (1989) 403.
- [23] T. Schäfer and E. Shuryak, Rev. Mod. Phys. 70 (1998) 323 and references therein.
- [24] F. Niedermayer, private communication.
- [25] A. Yung, “Valley Method for Instanton-Induced Effects in Quantum Field Theory”, in Proc. ICTP 1991 *Summer School on High Energy Physics and Cosmology*, p. 580. I. Balitsky and A. Schäfer, Nucl. Phys. B 404 (1993) 639.

- [26] P. J. Braam and P. van Baal, Commun. Math. Phys. 122 (1989) 267.
- [27] M. García Pérez, A. González-Arroyo, J. Snippe and P. van Baal, Nucl. Phys. B413 (1994) 535.
- [28] M. García Pérez and P. van Baal, Nucl. Phys. B429 (1994) 451.
- [29] P. de Forcrand G. Schierholz, H. Schneider and M. Teper, Phys. Lett. B160 (1985) 137.
- [30] C. Michael and M. Teper, Phys. Lett. B199 (1987) 95, Nucl. Phys. B305 (1988) 453; J. Fingberg et al., Nucl. Phys. B392 (1993) 493.
- [31] D. J. R. Pugh and M. Teper, Phys. Lett. 224B (1989) 159.
- [32] E. Seiler and I.-O. Stamatescu, preprint MPI-PAE/PTh 10/87.